Asia-Pac. J. Atmos. Sci., 52(2), 171-189, 2016
DOI:10.1007/s13143-016-0018-8
pISSN 1976-7633 / eISSN 1976-7951

Projections of High Resolution Climate Changes for South Korea Using Multiple-Regional Climate Models Based on Four RCP Scenarios. Part 2: Precipitation

Seok-Geun Oh[1], Myoung-Seok Suh[1], Young-Suk Lee[1], Joong-Bae Ahn[2], Dong-Hyun Cha[3], Dong-Kyou Lee[4], Song-You Hong[5], Seung-Ki Min[6], Seong-Chan Park[7], and Hyun-Suk Kang[8]

[1]*Department of Atmospheric Sciences, Kongju National University, Kongju, Korea*
[2]*Department of Atmospheric Sciences, Pusan National University, Busan, Korea*
[3]*School of Urban and Environmental Engineering, Ulsan National Institute of Science and Technology, Ulsan, Korea*
[4]*School of Earth and Environmental Sciences, Seoul National University, Seoul, Korea*
[5]*Korea Institute of Atmospheric Prediction Systems, Seoul, Korea*
[6]*School of Environmental Science and Engineering, Pohang University of Science and Technology, Pohang, Korea*
[7]*Korea Meteorological Administration, Seoul, Korea*
[8]*National Institute of Meteorological Sciences, Jeju, Korea*

(Manuscript received 30 October 2015; accepted 12 April 2016)

Abstract: Precipitation changes over South Korea were projected using five regional climate models (RCMs) with a horizontal resolution of 12.5 km for the mid and late 21st century (2026-2050, 2076-2100) under four Representative Concentration Pathways (RCP) scenarios against present precipitation (1981-2005). The simulation data of the Hadley Centre Global Environmental Model version 2 coupled with the Atmosphere-Ocean (HadGEM2-AO) was used as boundary data of RCMs. In general, the RCMs well simulated the spatial and seasonal variations of present precipitation compared with observation and HadGEM2-AO. Equal Weighted Averaging without Bias Correction (EWA_NBC) significantly reduced the model biases to some extent, but systematic biases in results still remained. However, the Weighted Averaging based on Taylor's skill score (WEA_Tay) showed a good statistical correction in terms of the spatial and seasonal variations, the magnitude of precipitation amount, and the probability density. In the mid-21st century, the spatial and interannual variabilities of precipitation over South Korea are projected to increase regardless of the RCP scenarios and seasons. However, the changes in area-averaged seasonal precipitation are not significant due to mixed changing patterns depending on locations. Whereas, in the late 21st century, the precipitation is projected to increase proportionally to the changes of net radiative forcing. Under RCP8.5, WEA_Tay projects the precipitation to be increased by about +19.1, +20.5, +33.3% for annual, summer and winter precipitation at 1-5% significance levels, respectively. In addition, the probability of strong precipitation (≥ 15 mm d^{-1}) is also projected to increase significantly, particularly in WEA_Tay under RCP8.5.

Key words: Future precipitation changes, five regional climate models, ensemble, RCP scenarios, South Korea

1. Introduction

Reliable high-resolution information concerning change in precipitation is an imperative requirement of various communities dealing with precipitation in areas, such as water management, hydrology, and agriculture. Its availability is necessary to develop suitable adaptation and mitigation strategies. Many studies using observations and climate models reported that the global warming is accelerated by anthropogenic factors (e.g., Giorgi and Mearns, 1999; Easterling et al., 2000; Suh and Lee, 2004; Bao, 2012; IPCC, 2013). In addition, some studies have reported that the frequency of occurrence of abnormal precipitation events, such as droughts and floods, has recently increased due to global warming (e.g., Easterling et al., 2000; Klein Tank and Können, 2003; Kim et al., 2009; Yoon et al., 2012; IPCC, 2013; Jeong et al., 2014). Therefore, in order to adapt for these changes in precipitation and organize efficient countermeasures, studies that improve the reliability of future climate change information are needed.

Since 1995, the global climate modeling groups have performed international collaborative studies, such as the CMIP (Coupled Model Intercomparison Project), to evaluate the performance of various global climate models (GCMs) for the present climate and the uncertainties of future climate information projected by them (e.g., Meehl *et al.*, 2000; Bao, 2012; Taylor et al., 2012). The regional climate modeling groups have also performed various international collaborative projects for certain areas of interest (e.g., "RMIP" in Asia, Fu et al., 2005; "PRUDENCE" in Europe, Jacob et al., 2007; "ENSEMBLES" in Europe, van der Linden and Mitchell, 2009; "NARCCAP" in North America, Wang et al., 2009). In particular, since 2009, the CORDEX (COordinated Regional Climate Downscaling, http://www.cordex.org/) project which utilized the common simulation environment (e.g., domain, simulation period, climate change scenarios, etc.), with CMIP5 (CMIP phase 5) has progressed actively all over the world. As a result, various global and regional climate data based on four RCP (Representative Concentration Pathway) scenarios (Moss et al., 2008; Van Vuuren et al., 2011), as new climate change

Corresponding Author: Myoung-Seok Suh, Department of Atmospheric Sciences, Kongju National University, Gongju 32588, Korea.
E-mail: sms416@kongju.ac.kr

scenario developed and recommended by IPCC (Intergovernmental Panel on Climate Change), have been produced (e.g., Bao, 2012; Taylor et al., 2012; Giorgi et al., 2012; Zou and Zhou, 2013; Lee et al., 2014; Oh et al., 2014).

Although GCMs and regional climate models (RCMs) are powerful tools to project future climate changes, their simulation data have considerable uncertainties due to various internal and external factors, such as the inaccuracy of the boundary data and the simplification of physics parameterizations, etc. (e.g., Giorgi and Mearns, 1999; Jacob et al., 2007; Dodla et al., 2013). The simulation of precipitation related with complicated interaction of various climate elements (e.g., wind, temperature, relative humidity, etc.), has particularly larger uncertainties than the other climate elements such as temperature and wind, etc. (Giorgi and Means, 1999; Lee and Suh, 2000; Dodla et al., 2013; Oh et al., 2014). Considering the understanding of water cycle around the globe is very important to human life, the studies which can improve the precipitation information simulated by the GCMs and RCMs are needed.

It is well known that multi-model ensembles can reduce the uncertainty and improve the reliability of global or regional climate information (e.g., Krishnamurti et al., 1999; Giorgi and Mearns, 2002; Yun et al., 2005; Casanova and Ahrens, 2009; Suh et al., 2012; Oh and Suh, 2015; Li et al., 2016). In the meantime, the multi-model ensemble studies have been conducted in global climate modeling and numerical weather forecasting groups that have relatively large simulation dataset. Some regional climate modeling groups have also conducted multi-model ensemble studies, using vast amounts of simulated regional climate information with the enhanced computing resource (e.g., Giorgi and Mearns, 2002; Casanova and Ahrens, 2009; Suh et al., 2012; Oh and Suh, 2015). However, despite increasing computational resources, there are still various limitations for utilizing regional climate information forced by multi-GCMs in ensemble. For this reason, Oh and Suh (2015) developed the Weighted Ensemble Averaging using Taylor (2001) skill score (WEA_Tay) to produce reliable climate information even under a small number of ensemble members. They reported that WEA_Tay showed relatively good skills in both accuracy and reliability compared with existing ensemble methods.

Recently, the National Institute for Meteorological Sciences (NIMS) of the Korea Meteorological Administration (KMA) has produced the present 25-yr (1981-2005) and the future 45-yr (2006-2050) climate based on RCP4.5 and 8.5 scenarios over CORDEX East Asian region using five RCMs, with the intention of establishing national standard scenarios of climate change (https://cordex-ea.climate.go.kr/; Suh et al., 2012; Lee et al., 2014; Oh et al., 2014). However, it has a fundamental limit in spatial resolution (50 km) for direct utilizations in the various application fields which require more fine-scale climate information such as hydrology and agriculture. Therefore, they have also produced fine-scale (12.5 km resolution) climate change data sets covering about 110 years (1981-2010, 2021-2100 under four RCP scenarios) over the Northeast Asian region focusing on the Korean Peninsula, using the five RCMs (e.g., KMA, 2015; Hong and Ahn, 2015).

As a companion work for the study by Suh et al. (2016), this work aims at projecting the characteristic of future changes in precipitation for the mid (2026-2050) and late (2076-2100) 21st century under the four RCP scenarios (2.6, 4.5, 6.0, and 8.5) over the Northeast Asian region focusing on South Korea. In addition, to improve the reliability of precipitation information during present and future periods, we also present the ensemble results produced by a simple arithmetic mean and WEA_Tay. The next section of this paper briefly explains the boundary data, the five RCMs and experimental design, and the ensemble methods used in this study. And then, the analysis results for the performance of present precipitation and the precipitation change for the mid and late 21st century according to the four RCP scenarios are presented in Section 3. Finally, the outcomes of this study are summarized in Section 4.

2. Models and experimental setups

a. Lateral boundary condition

In this study, we used the simulation data of the Hadley Centre Global Environmental Model version 2 coupled with the Atmosphere-Ocean (HadGEM2-AO) under the four RCP scenarios (Baek et al., 2013), provided by the NIMS/KMA, as lateral boundary data for five RCMs. In order to stabilize and understand the internal variability of model, the pre-industrial control simulation was performed for 400 years under the fixed values of greenhouse gases in 1860 (Baek et al., 2013). Subsequently, a historical run was performed up to 2005 by using the final output of the pre-industrial control simulation as the initial condition for the atmosphere and the ocean. In this simulation of the past climate, forcing factors inherent to greenhouse gases, aerosols, the ozone, volcanic eruptions, and the solar activity were taken into account. The projection of the future climate up to 2100 was performed under the four RCP scenarios by using the 2005 output of the historical run as the initial condition. Details of HadGEM2-AO are given by Collins et al. (2011), and detailed descriptions on these experiments are shown in Baek et al. (2013). In this study, to perform RCM simulations, the sea surface temperature (SST) and atmospheric variables (e.g., u and v components, temperature, moisture, geopotential height, etc.) of HadGEM2-AO were updated by every six hours.

b. RCMs and experiment design

The RCM domain covers the Northeast Asian region that is centered on 37.5°N and 127.5°E at 12.5 km grid spacing, including the Korean Peninsula (Fig. 1), as described in the paper of Suh et al. (2016). The five RCMs used to simulate the present and future climate over the Northeast Asian region are: the Seoul National University Regional Climate Model (SNURCM, Lee et al., 2004), the Weather Research and

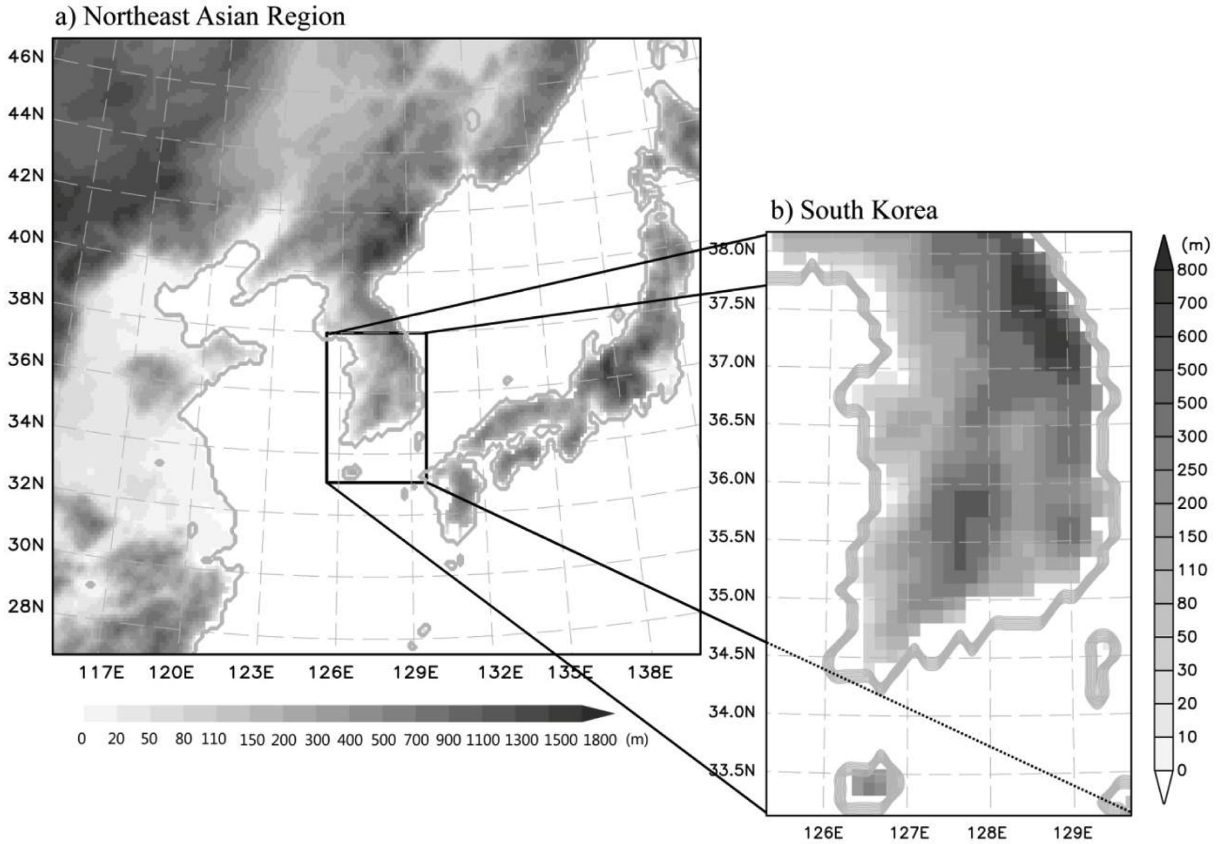

Fig. 1. The a) Northeast Asian region and b) South Korea (Lat.: 33-39°N, Lon.: 125-130°E) indicate the simulation domain and the detailed analysis region used in this study, respectively. This figure is same as Fig. 1 in Suh et al. (2016) as our companion study.

Forecasting model version 3.4 (WRF3.4, Skamarock et al., 2005), the Regional Climate Model version 4.0 (RegCM4, Giorgi et al., 2012), the Global/Regional Integrated Model system (GRIMs, Hong et al., 2013), the Hadley Centre Global Environment Model version 3 regional atmospheric version (HadGEM3-RA, Hewitt et al., 2010). The detailed information concerning the development of each RCM can be found in the respective references cited above.

The parameterizations of physical processes play important roles in regional climate simulations. In particular, the convective parameterization scheme is very relevant for the simulation of precipitation (e.g., Kain and Fritsch, 1993; Kerkhoven et al., 2006; Dodla et al., 2013). In this experiment, SNURCM and WRF used the Kain-Fritsch II scheme (Kain and Fritsch, 1993; Kain, 2004). RegCM4 and HadGEM3-RA used the MIT-Emanuel (1991) scheme and the revised mass flux convection scheme (Gregory and Rowntree, 1990), respectively. GRIMs used the Simplified Arakawa-Schubert (SAS) scheme (Hong and Pan, 1998) with Convective Momentum Transport (CMT, Byun and Hong, 2007). These convective parameterization schemes were selected, because their performance have been evaluated through previous RCM studies for CORDEX-East Asia region and the Korean Peninsula (e.g., Suh et al., 2012; Sung et al., 2012; Lee et al., 2014; Oh et al., 2014; Jin et al., 2015). More detailed information concerning the configuration of five RCMs is presented in Table 2 in Suh et al. (2016). The performance of each model with similar simulation environment, is also found in previous studies (e.g., Suh et al., 2012; Sung et al., 2012; Lee et al., 2014; Oh et al., 2014; Jin et al., 2015).

Regional climate simulations of four RCMs (RegCM4, GRIMs, SNURCM, and WRF) were conducted for the present 32 years (1979-2005 and 2006-2010 under RCP8.5) and the future 82 years (2019-2100) based on the four RCP scenarios (2.6, 4.5, 6.0, and 8.5). HadGEM3-RA simulation performed by NIMS/KMA was continuously conducted for the 122 years (1979-2100), unlike the other four RCMs. The concentrations of greenhouse gases (GHG) based on four RCP scenarios were applied in simulation after the year 2005. The GHG concentrations which are taken from the RCP scenarios data group (http://www.pik-potsdam.de/~mmalte/rcps/), are time-varying during the RCM simulations. To project future climate changes against the present climate, the present climate was set as the average climate for a 25-yr period from 1981 to 2005, and the mid and late 21st century future climate were set as the average climate for two 25-yr periods from 2026 to 2050 and from 2076 to 2100, respectively. The performances of five RCMs for the present precipitation were validated using APHRODITE (Asian Precipitation High Resolved Observational Data Integration Towards Evaluation of water re-

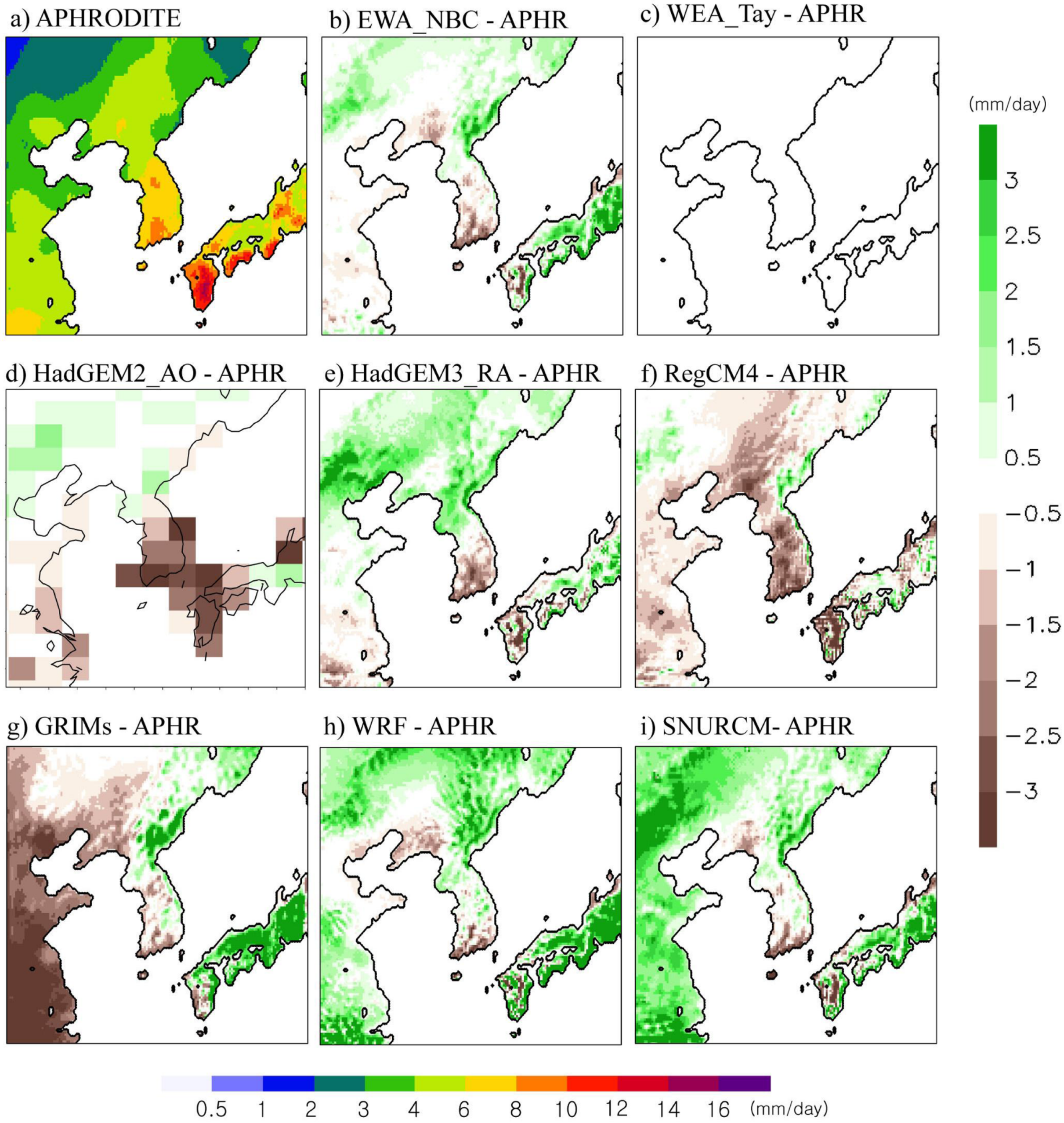

Fig. 2. Spatial distribution of summer (JJA) mean precipitation (mm d^{-1}) of (a) APHRODITE (APHR), (b to i) differences of summer mean precipitation (mm d^{-1}) between each simulation and APHR for the present 25-yr period (1981-2005).

sources) precipitation data based on surface observations. The APHRODITE precipitation data are the daily gridded precipitation data with a high spatial resolution (about 25 km) but are only available for land areas (Yatagai et al., 2012). To evaluate or compare the performance of the five RCMs for the present precipitation (1981-2005), the APHRODITE precipitation data is interpolated to the RCMs grid points using a bilinear interpolation. All evaluations and projections for the present and future precipitation were performed using the monthly averaged datasets.

c. Ensemble methods

Various types of ensemble methods using simulation data from multiple Numerical Weather Prediction (NWP) models, GCMs, and RCMs generally outperform the result derived from the single best model (e.g., Krishnamurti et al., 1999; Giorgi and Mearns, 2002; Yun et al., 2005; Casanova and Ahrens, 2009; Suh et al., 2012). In this study, we used two types of ensemble methods: equal weighted averaging without bias correction (EWA_NBC) and weighted ensemble averaging based on Taylor's skill score (WEA_Tay) (Taylor, 2001). As

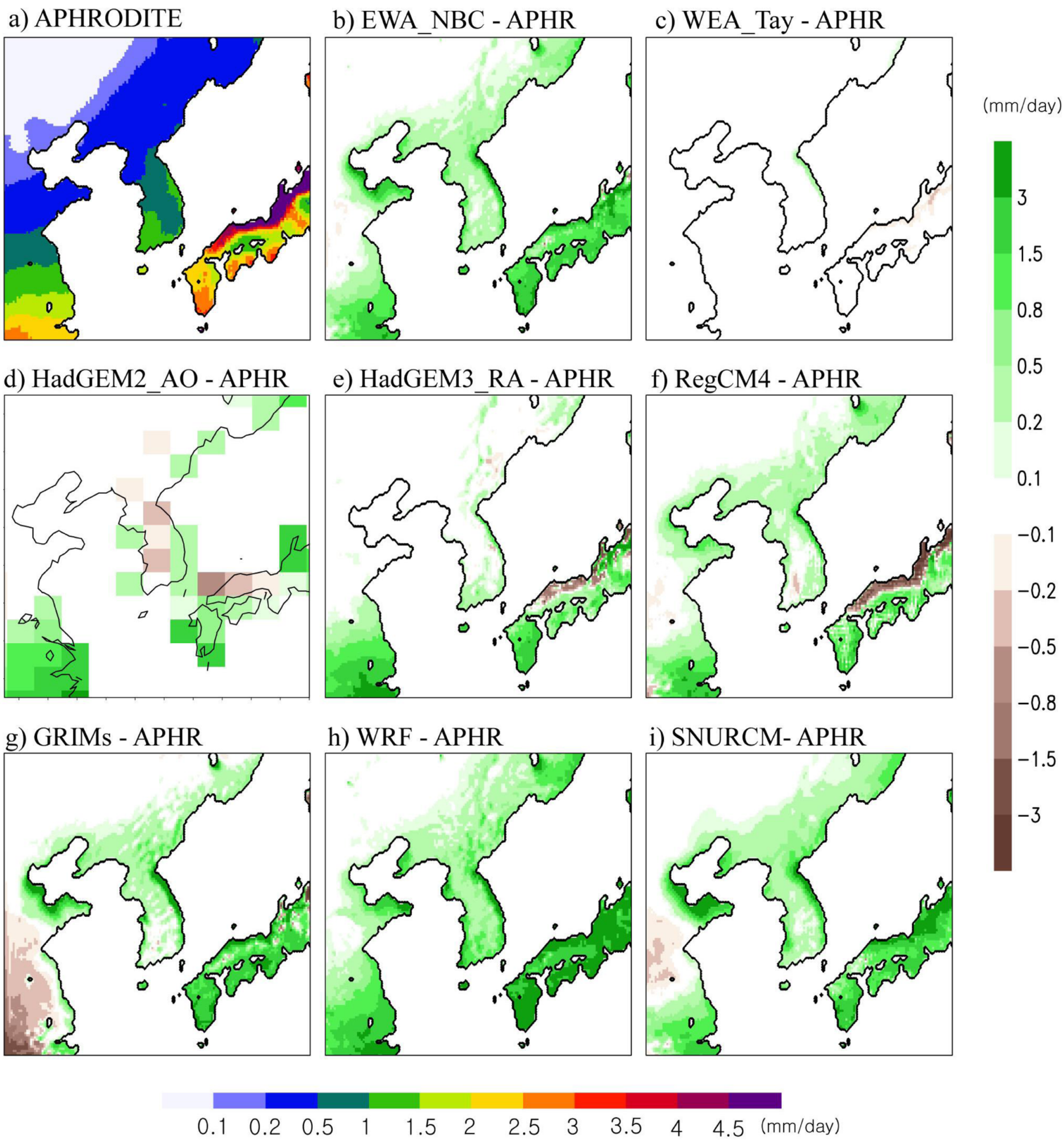

Fig. 3. Same as Fig. 2 except for winter (DJF) mean precipitation (mm d^{-1}).

an arithmetic average, EWA_NBC is widely used in NWP and GCM communities that have a relatively large number of ensemble members. The advantage of this method is that it is easier to use because observation data are not required in the ensemble averaging process. Previous studies have shown that EWA_NBC can improve the simulation skills compared to a single model, especially when the ensemble members are independent of each other (e.g., Palmer et al., 2004; Christensen et al., 2010).

The WEA_Tay method, introduced by Oh and Suh (2015), utilizes Taylor's skill score as the weight of each model. Taylor's skill score is a very useful measure for the evaluation of complex global or regional climate models (Taylor, 2001). Previous studies have utilized this score to compare the performance of various types of models (e.g., Van der Linden and Mitchell, 2009; Park et al., 2015). This score is based on the combination of the correlation and normalized standard deviation (modeled standard deviation divided by observed standard deviation) between simulated and observed data. To produce the ensemble precipitation in this study, we used Taylor's skill score calculated by temporal correlation and normalized standard deviation at each RCM grid point. For a detailed explanation of the WEA_Tay method including equations, please see Oh and Suh (2015) and Suh et al. (2016). The same weight values of each RCM were used for ensemble projection of future precipitation (2021-2100).

3. Results

a. Performance of precipitation for the present climate

Figures 2 and 3 show the spatial distribution of APHRODITE and the differences of HadGEM2-AO, five RCMs, and two ensemble methods compared with APHRODITE for summer (JJA) and winter (DJF) mean precipitation over the Northeast Asian region during the present climate (1981-2005). To compare the performances for precipitation clearly, the color scales for summer and winter are presented differently. Generally, the precipitation in the Northeast Asian region is mostly affected by persistent rainbands associated with the East Asian summer and winter monsoon. Therefore, the APHRODITE results depict large amounts of precipitation located in southern area of the Korean Peninsula, Japan, and Southeast China (Figs. 2a and 3a). The summer (winter) mean precipitation amounts to 6-14 (1-4.5) mm d^{-1} around South Korea and Japan and to 2-6 (0.1-0.5) mm d^{-1} around northeastern China due to the seasonal march of the East Asian summer (winter) monsoon. Compared with APRHODITE, HadGEM2-AO simulates well the amount of summer and winter precipitation, although it significantly underestimates the summer precipitation by about −1 to −3 mm d^{-1} around South Korea and Kyushu, Japan.

In general, the characteristics of summer and winter precipitation simulations from five RCMs are similar to those of HadGEM2-AO, but their performances are different depending on the regions, seasons, and the RCMs. For summer precipitation, all five of the RCMs considerably reduce the dry biases over South Korea and Kyushu, Japan produced by HadGEM2-AO. In particular, the GRIMs, WRF, and SNURCM show reasonable simulations with small dry and wet biases about ± 0.5 mm d^{-1} in South Korea compared to HadGEM2-AO, although they show significant wet bias of about +1 to +3 mm d^{-1} in the Japanese Islands. The HadGEM3-RA and RegCM4 show relatively large dry biases of about −0.5 to −2 mm d^{-1} over South Korea in comparison to the other RCMs; however, their performance is better in the Japanese Islands than the other RCMs. For winter precipitation, all five of the RCMs simulate a similar bias pattern to HadGEM2-AO, but they show larger wet biases in most of the RCM domain, particularly over South Korea and Japan in the SNURCM and WRF models. Precipitation is consistently overestimated using the Kain-Fritsch II scheme (Figs. 2h, 2i, 3h, and 3i; Kain and Fritsch, 1993; Kain, 2004), which was used in WRF and SNURCM simulations and has been reported in many previous studies (e.g., Kerkhoven et al., 2006; Litta et al., 2007; Dodla et al., 2013). However, the performance of the GRIMs for precipitation is clearly dependent on the region. While more

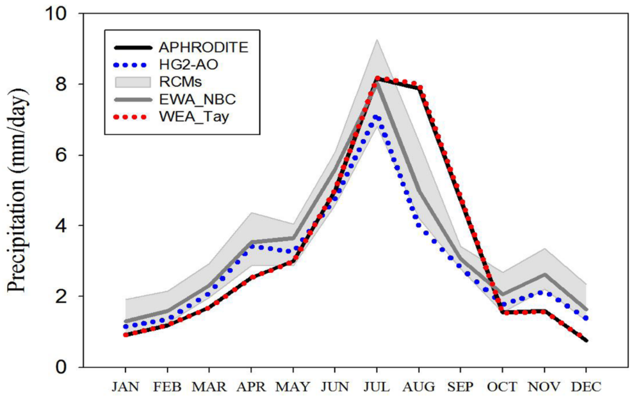

Fig. 4. Seasonal variation of 25-yr (1981-2005) averaged monthly mean precipitation (mm d^{-1}) over South Korea (Lat.: 33-39°N, Lon.: 125-130°E). The black solid line, blue dotted line, grey solid line, and red dotted line indicate the APHRODITE, HadGEM2-AO (HG2-AO), EWA_NBC, and WEA_Tay, respectively. The grey shading indicates the full range between the monthly mean precipitation simulated by the RCM results.

precipitation is generally simulated in the east coast of the Korean Peninsula and in Japan, much less precipitation is simulated in the western coast of the Korean Peninsula and in southeast and northeast regions of China. These differences in precipitation simulations can be partly explained by the differences in convective parameterization schemes, which significantly affect the RCM simulation of precipitation.

In general, EWA_NBC method reproduces summer precipitation well in most of the RCM domain because the wet and dry biases in RCMs are offset. However, the excessive precipitation is maintained in most of the RCM domain for winter when all RCMs show wet biases systematically. In contrast, WEA_Tay better corrects the wet and dry biases that appear in the five RCM simulations of summer and winter. As a result, it well produces similar spatial distributions as well as precipitation amount compared with APHRODITE.

The seasonal variation of 25-yr (1981-2005) averaged monthly mean precipitation (mm d^{-1}) over South Korea (Lat.: 33-39°N, Lon.: 125-130°E) is shown in Fig. 4. The five RCMs capture well the seasonal variation of precipitation with maximum in summer and minimum in winter. However, they overestimate winter precipitation and underestimate summer precipitation, compared with APRHODITE. As a result, the amplitude of the seasonal variation of precipitation is relatively underestimated. These characteristics are considerably affected by the performance of HadGEM2-AO. In summer, the significant underestimation of precipitation over South Korea is associated with shifted monsoon circulations in HadGEM2-AO, such as the weakened simulation of low-level southwesterly winds caused by the weakened low-pressure system around the Korean Peninsula (Oh et al., 2011). This southward shift of the monsoonal front during summer is also associated with a cold SST bias in HadGEM2-AO (Park et al., 2015). However, the five RCMs simulate more precipitation in summer than HadGEM2-AO, although they simulate the weakened evolution

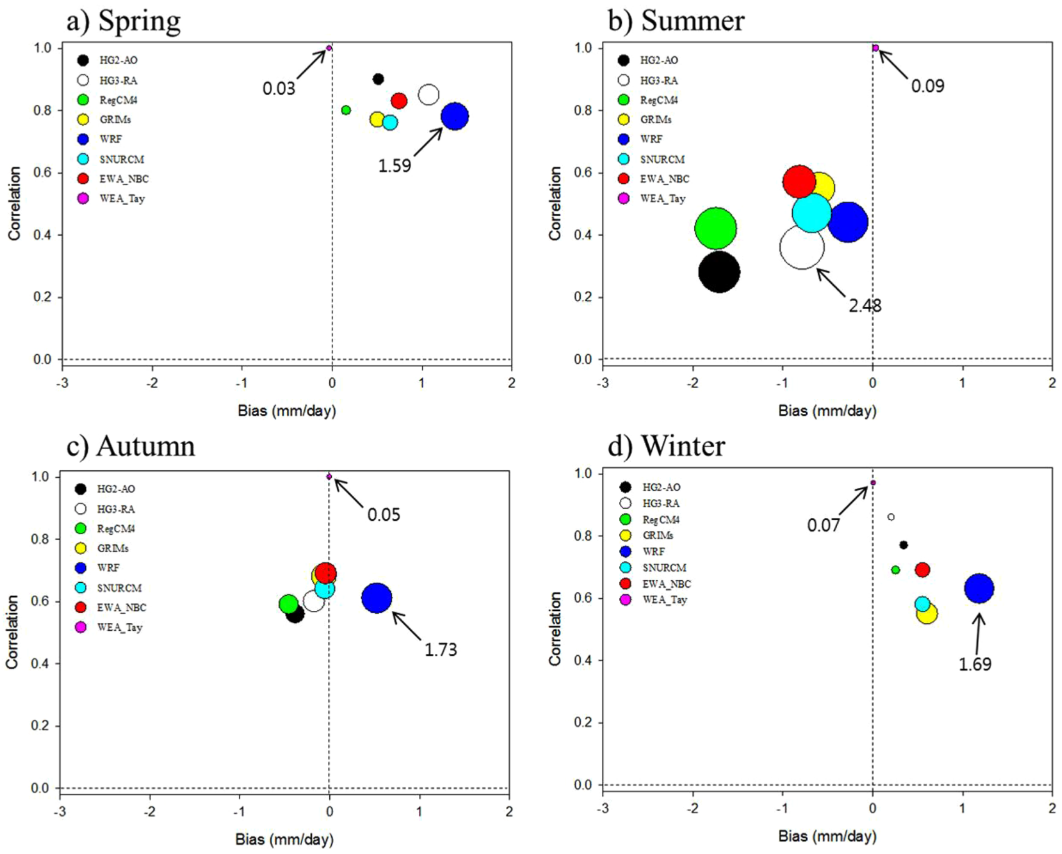

Fig. 5. BCR (Bias, Correlation and RMSE) diagram for seasonal mean precipitation (mm d^{-1}) over South Korea (Lat.: 33-39°N, Lon.: 125-130°E) during the present 25-yr period (1981-2005).

of the East Asian summer monsoon. It indicates that RCMs with high resolution compared to GCM can reasonably reproduce the characteristic of summer precipitation which occurs by the combined processes of synoptic scale (monsoon) and mesoscale convective system in this region. EWA_NBC relatively reduces the wet and dry biases of RCMs, but wet bias in winter and dry bias in summer still remain. On the other hand, WEA_Tay well corrects the different simulation skills of five RCMs according to the seasons, dry and wet biases for summer and winter, respectively.

Figure 5 shows the BCR (Bias, Correlation, and RMSE) diagram which synthetically summarized the performances of all models and two ensemble averages for seasonal mean precipitation over South Korea (Lat.: 33-39°N, Lon.: 125-130°E) during the present period (1981-2005). In general, the performances of RCMs for precipitation are different depending on the models and the seasons. The largest root mean square error (RMSE) and the lowest spatial correlation are found in summer when the precipitation occurs mostly by mesoscale weather systems. On the other hand, the lowest RMSE and highest spatial correlation are found in spring and winter when precipitation occurs mostly by synoptic weather systems. In terms of bias, the autumn precipitation is well simulated, but wet biases (dry biases) in spring and winter (summer) precipitation are clearly found in all RCMs. EWA_NBC slightly improves the performance in terms of bias, RMSE, and spatial correlation compared with the other RCMs and HadGEM2-AO, in particular in summer and autumn. On

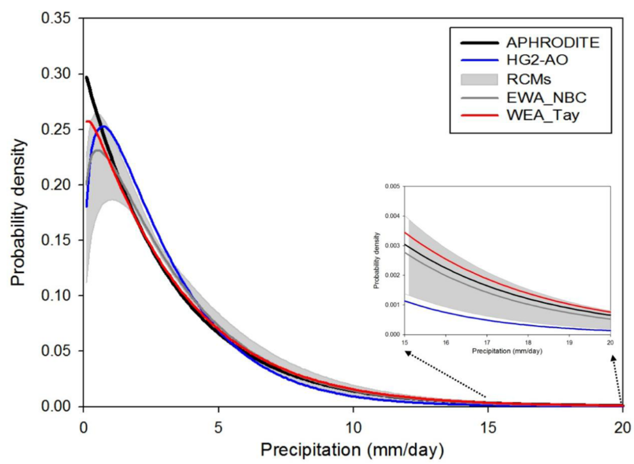

Fig. 6. Probability density function of monthly averaged precipitation (mm d^{-1}) over the South Korea (Lat.: 33-39°N, Lon.: 125-130°E) for the present climate (1981-2005). The black solid line, blue solid line, grey solid line, and red solid line indicate the APHRODITE, HadGEM2-AO (HG2-AO), EWA_NBC, and WEA_Tay, respectively. The grey shading is the full range of the regional climate model results.

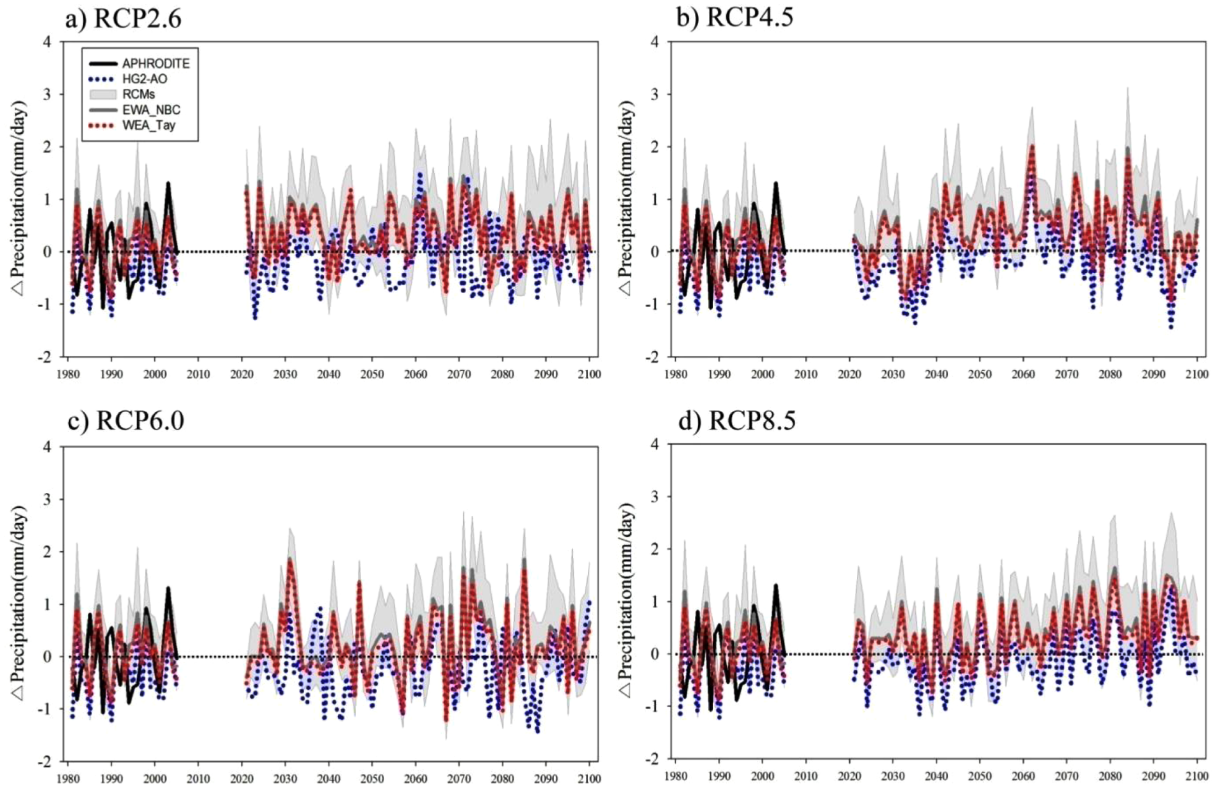

Fig. 7. Interannual variations of annual precipitation anomalies (mm d^{-1}) area-averaged for South Korea (Lat.: 33-39°N, Lon.: 125-130°E) during the present climate (1981-2005) and the future climate (2021-2100) over South Korea according to the RCP scenarios.

the other hand, WEA_Tay well corrects the different model biases toward observation, resulting in a good performance in terms of bias, RMSE, and spatial correlation.

Figure 6 shows the probability density function (PDF) of monthly averaged precipitation in all grid points within South Korea (Lat.: 33-39°N, Lon.: 125-130°E) for the present period (1981-2005). HadGEM2-AO underestimates the frequency in precipitation intensity from 0.1 to 2.0 mm d^{-1}, whereas it overestimates the frequency in precipitation intensity from 2.0 to 5.0 mm d^{-1}. These characteristics are similar in the result of five RCMs, in particular appearing much stronger in WRF. In addition, WRF significantly overestimates the frequency of occurrence of precipitation stronger than 5 mm d^{-1}, compared with APHRODITE. Therefore, the PDFs between RCMs for all precipitation intensity show broad range. As shown in many previous studies (e.g., Gu et al., 2012; Ham et al., 2015; Park et al., 2015), all RCMs perform better than HadGEM2-AO in the simulation of strong precipitation. This may indicate that RCMs with high resolution can reproduce more extreme precipitation events than GCMs with low resolution. This can be regarded as the 'added value' of regional dynamic downscaling (Giorgi and Mearns, 1999; Gu et al., 2012; Ji and Kang, 2014; Ham et al., 2015; Park et al., 2015). Although the PDF of EWA_NBC shows a mismatch with APRHODITE systematically, it shows a good performance in most of the precipitation intensity, compared with single RCM, in particular in strong precipitation. Regarding WEA_Tay, although the frequency of occurrence of precipitation intensity from 0.1 to 2.0 mm d^{-1} (over 2 mm d^{-1}) is slightly underestimated (overestimated), the PDF of WEA_Tay is close to that of APHRODITE. It indicates that spatial and temporal variations in precipitation, the amount of precipitation, and the frequency of binned precipitation intensity over South Korea can be corrected using WEA_Tay.

b. Projection of future precipitation changes

Figure 7 shows the anomalies (mm d^{-1}) of area-averaged annual precipitation over South Korea (Lat.: 33-39°N, Lon.: 125-130°E) for the present climate (1981-2005) and the future climate (2021-2100) according to the four RCP scenarios. The averaged value of the APHRODITE precipitation for the present period (1981-2005) is used as reference data. In general, WEA_Tay significantly reduces the systematic errors that are evident in the simulations of RCMs, and produces precipitation information similar to that of APHRODITE in terms of precipitation amount. Unlike the temperature result in Suh et al. (2016), the trends for annual mean temperature according to the four RCP scenarios are not clear. Under RCP2.6 and RCP6.0, the annual mean temperature does not follow any clear trend. On the other hand, under RCP4.5, the precipitation anomalies (mm d^{-1}) tend to increase around +0.5 mm d^{-1} yr^{-1}

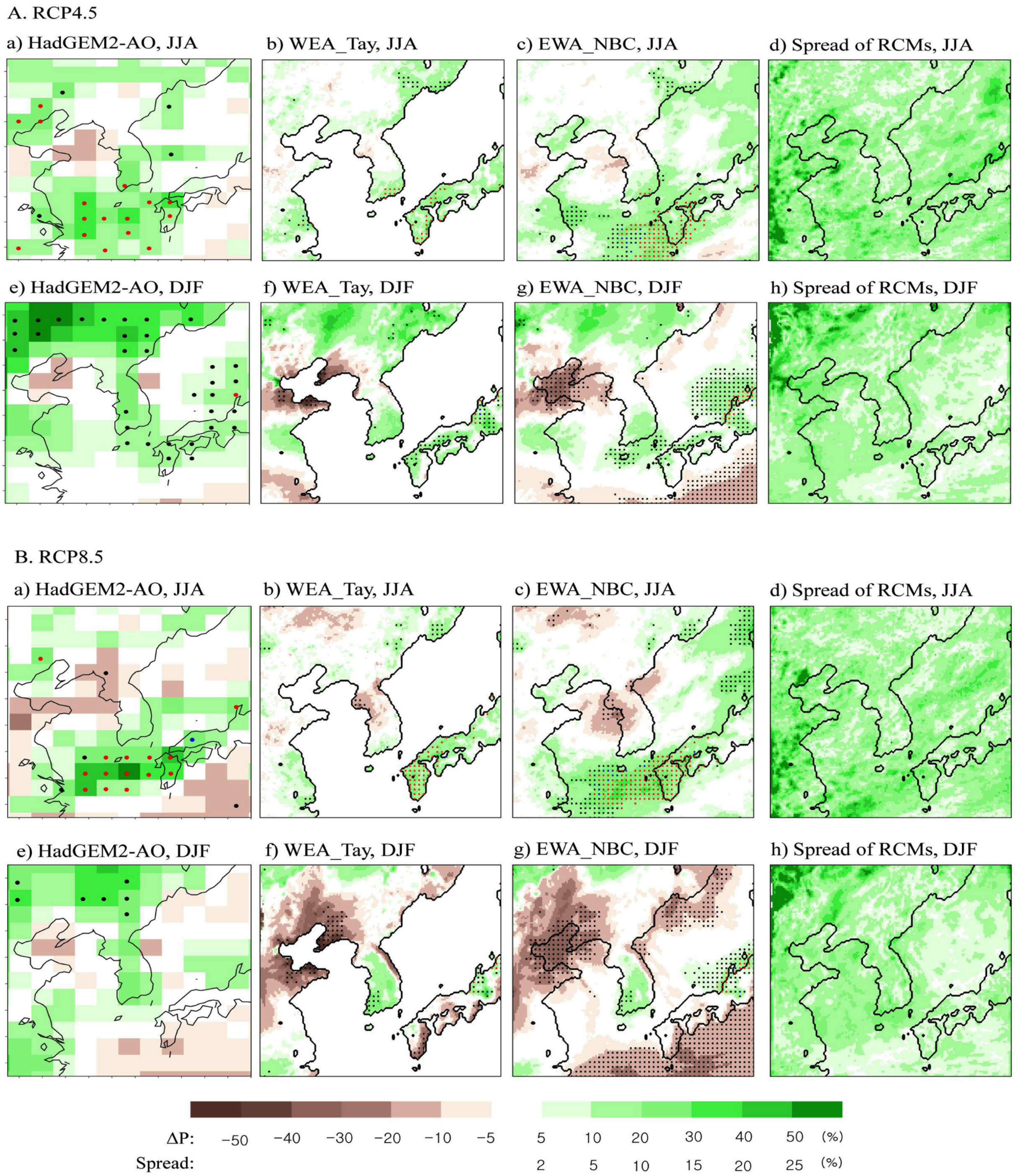

Fig. 8. Spatial distribution of projected summer (JJA) and winter (DJF) mean precipitation changes (%) during the mid-21st (2026-2050) century compared to the modeled present (1981-2005) climate based on the RCP4.5 and 8.5 scenarios. The regions with black, blue, and red dot indicate precipitation changes with 10%, 5%, and 1% significance level of t-test, respectively.

from 2040 to 2090. However, after 2090, the precipitation anomalies (mm d^{-1}) show around 0 mm d^{-1} yr^{-1} again. Under RCP8.5, the precipitation anomalies (mm d^{-1}) show around 0 mm d^{-1} yr^{-1} up to 2060, but a steadily increasing trend is dominant after 2060. Therefore, it can be estimated that the annual precipitation will be increased significantly in the late 21st century under RCP8.5. Additional analysis concerning changes of spatial and temporal variations, as well as the frequency of occurrence according to the precipitation intensity in the mid (2026-2050) and late (2076-2100) 21st century was pursued further in the subsection below.

(1) Precipitation changes in the mid-21st century

Figure 8 shows changes (%) in summer (JJA) and winter (DJF) mean precipitation during the mid-21st century (2026-2050) compared with the present climate (1981-2005) based on RCP4.5 and RCP8.5 scenarios. Generally, the magnitude of precipitation change was slightly different according to the seasons and the RCP scenarios. Under RCP4.5, HadGEM2-AO projects that the precipitation in East China Sea and in northeastern China will be significantly increased by about +10% to +30% and +30% to +50% within the 1% or 10% significance levels during summer and winter, respectively. These precipitation changes similarly appear in the results of the multi-RCM ensembles. However, unlike HadGEM2-AO, the multi-RCM ensembles project a significant decrease in precipitation between −10% and −30% around the Gulf of Pohai and the Southern Ocean in Japan during winter. In addition, the precipitation increases in northeastern China during summer and winter are less than those produced by HadGEM2-AO and are not statistically significant. Under RCP8.5, the precipitation changes of multi-RCM ensembles are generally similar to those under RCP4.5. However, relatively large precipitation decreases with a 10% significance level are found in the middle of the Korean Peninsula during summer and in the Gulf of Pohai and the Southern Ocean in Japan during winter. Compared to the results of Zou and Zhou (2013), which projected future (2016-2040) precipitation changes over China using RegCM3 forced by another GCM (Flexible Global Ocean-Atmosphere-Land system model Grid-point version 2, FGOALS-g2) under RCP8.5, the increases of precipitation around northeastern China in this study are relatively small and not significant. Generally, the inter-RCM spread appears similarly in most of the RCM domain regardless of season and RCP scenario, except for the northeastern China during winter. It indicates that the projection skills of five RCMs for precipitation are mostly similar in this RCM domain. A much greater increase in summer precipitation over South Korea is projected in the south, but a significant decrease is projected in the middle region, particularly under RCP8.5. This contrasting changing pattern indicates that the spatial variability of precipitation over South Korea will be intensified in the mid-21st century.

The amounts of change (mm d^{-1}) in seasonal mean precipitation over South Korea during the mid-21st century compared with the present climate according to the four RCP scenarios are summarized in Table 1. The ratio of relative change (%) is also presented in Table 1. The changes in seasonal mean

Table 1. Projection of precipitation changes (mm d^{-1}) during the mid-21st (2026-2050) century compared to the modeled present period (1981-2005) over South Korea (Lat.: 33-39°N, Lon.: 125-130°E) according to the RCP scenarios. The values in parenthesis indicate the ratio of relative change (%) of future precipitation against present precipitation.

Seasons	Scenarios	HadGEM2-AO	HadGEM3-RA	RegCM4	GRIMs	WRF	SNU RCM	EWA_NBC	WEA_Tay	Spread of RCMs
Annual	RCP2.6	**0.19*** **(6.4)**	0.23* (6.6)	0.28* (5.5)	0.13 (3.9)	0.37** (9.6)	0.29** (8.6)	**0.26**** **(7.7)**	**0.27**** **(8.9)**	**0.09** **(2.30)**
	RCP4.5	**0.00** **(0.0)**	0.10 (3.0)	0.19 (2.4)	0.11 (3.3)	0.31* (7.8)	0.21 (6.2)	**0.18** **(5.3)**	**0.19*** **(6.5)**	**0.09** **(2.34)**
	RCP6.0	**−0.01** **(−0.3)**	0.10 (2.7)	0.18 (2.0)	0.08 (2.4)	0.14 (3.5)	0.20 (5.9)	**0.14** **(4.2)**	**0.17** **(4.9)**	**0.05** **(1.55)**
	RCP8.5	**−0.01** **(−0.3)**	0.06 (1.5)	0.13 (0.3)	0.08 (2.4)	0.12 (3.0)	0.04 (1.2)	**0.09** **(2.4)**	**0.10** **(3.7)**	**0.04** **(1.05)**
Summer	RCP2.6	**−0.12** **(−2.3)**	0.29 (4.6)	0.33 (2.9)	0.08 (1.1)	0.45 (6.8)	1.08** (17.0)	**0.45** **(7.1)**	**0.46** **(7.2)**	**0.38** **(6.25)**
	RCP4.5	**−0.19** **(−3.6)**	0.26 (4.0)	0.21 (0.6)	0.10 (1.6)	0.45 (6.7)	0.69 (10.7)	**0.34** **(5.5)**	**0.38** **(6.1)**	**0.23** **(4.09)**
	RCP6.0	**−0.06** **(−1.1)**	0.05 (0.8)	−0.03 (−3.9)	−0.08 (−1.4)	−0.06 (−0.9)	0.48 (7.6)	**0.07** **(1.1)**	**0.17** **(2.5)**	**0.23** **(4.34)**
	RCP8.5	**−0.37** **(−7.1)**	−0.01 (−0.2)	−0.05 (−4.0)	−0.21 (−3.3)	−0.25 (−3.7)	−0.08 (−1.3)	**−0.12** **(−1.9)**	**−0.07** **(−0.3)**	**0.10** **(1.66)**
Winter	RCP2.6	**0.02** **(1.5)**	0.09 (8.7)	0.13 (6.3)	−0.02 (−1.3)	0.15 (7.0)	−0.09 (−6.0)	**0.05** **(3.3)**	**0.07** **(7.5)**	**0.10** **(6.30)**
	RCP4.5	**0.02** **(1.5)**	0.08 (7.0)	0.16 (7.9)	0.08 (5.8)	0.20 (9.3)	0.03 (2.0)	**0.11** **(7.3)**	**0.11** **(12.9)**	**0.07** **(2.77)**
	RCP6.0	**0.02** **(0.8)**	−0.04 (−3.5)	0.03 (−1.6)	−0.02 (−1.3)	−0.03 (−1.4)	−0.03 (−2.6)	**−0.02** **(−1.3)**	**−0.01** **(−2.2)**	**0.03** **(0.95)**
	RCP8.5	**0.00** **(0.0)**	0.11 (10.4)	0.17 (8.7)	−0.01 (−0.6)	0.20 (9.3)	0.00 (0.0)	**0.09** **(6.6)**	**0.10** **(10.8)**	**0.10** **(5.39)**

***Significance level: 1%, **Significance level: 5%, *Significance level: 10%

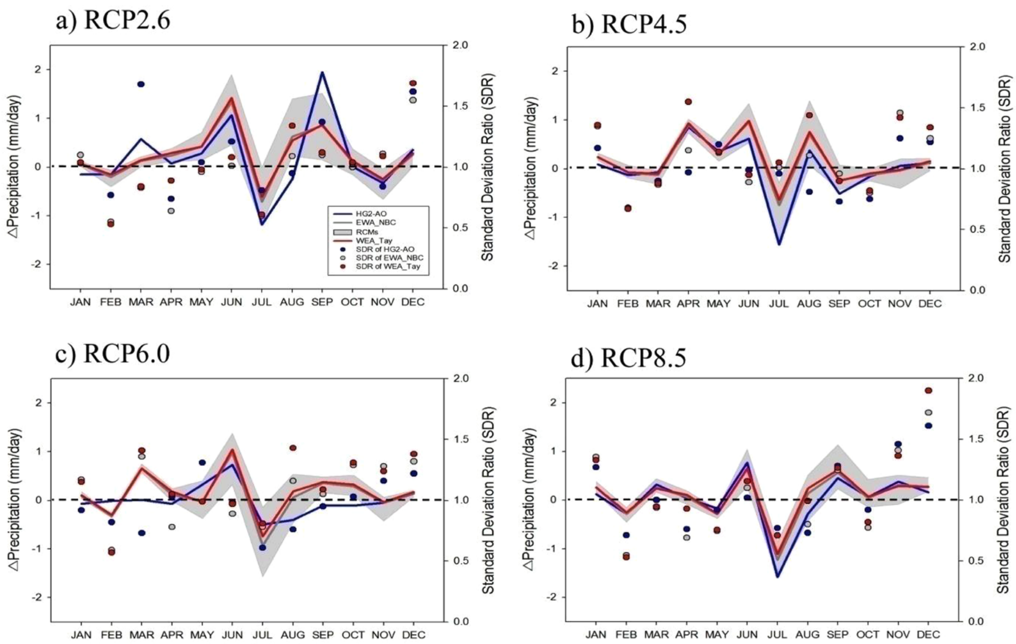

Fig. 9. Change of seasonal variation of monthly mean precipitation in the mid-21st century (2026-2050) over South Korea (Lat.: 33-39°N, Lon.: 125-130°E) compared to the modeled present period (1981-2005) according to the four RCP scenarios. The blue, grey, and red solid line indicate the HadGEM2-AO (HG2-AO), EWA_NBC, and WEA_Tay, respectively. The grey shading indicates full range of the regional climate model results. In addition, the circles denote the standard deviation ratio (standard deviation in future climate to standard deviation in present climate) for interannual variation of the monthly precipitation.

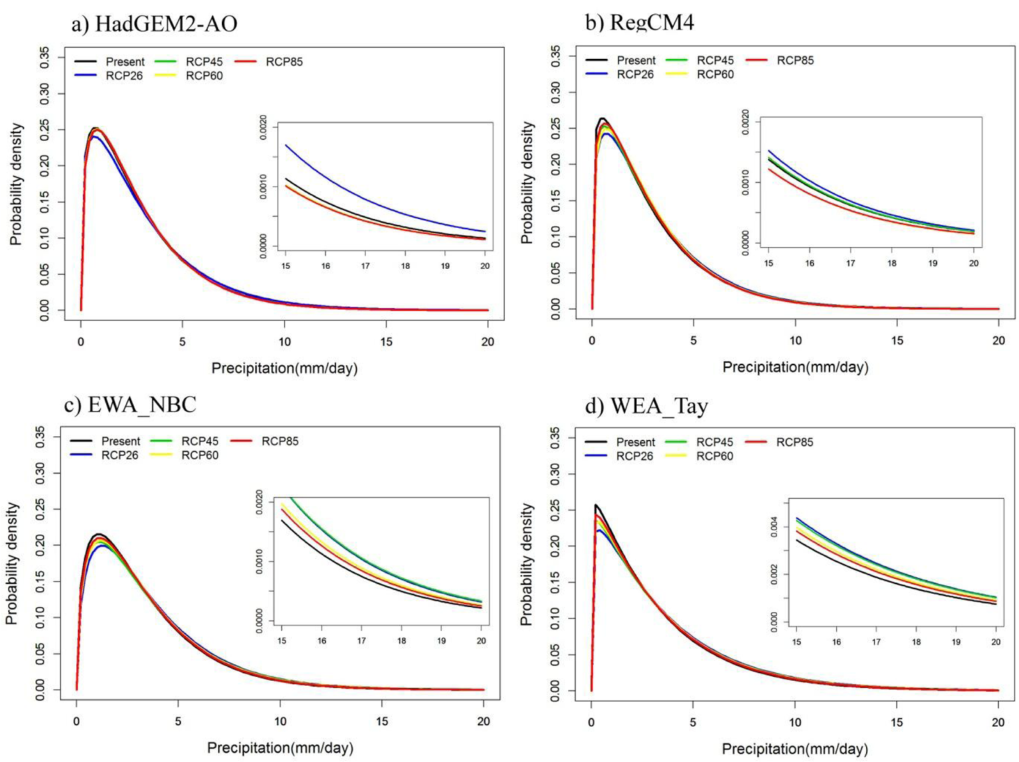

Fig. 10. Change of probability density function of monthly averaged precipitation (mm d^{-1}) in the mid-21st century (2026-2050) over South Korea (Lat.: 33-39°N, Lon.: 125-130°E) compared to the modeled present climate (1981-2005).

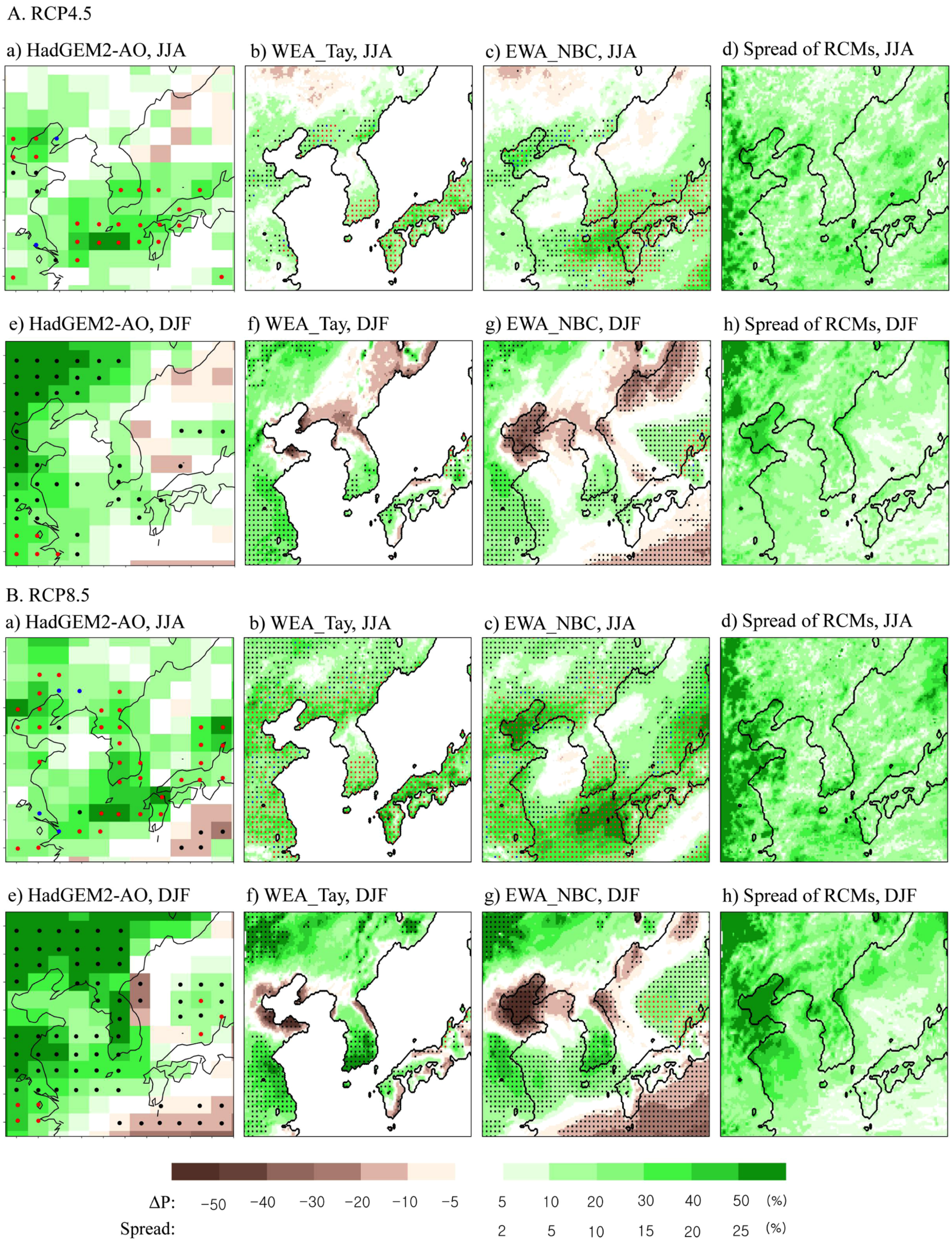

Fig. 11. Same as Fig. 8 except for the late 21st century (2076-2100).

precipitation over South Korea differ according to seasons, RCP scenarios, and models. Under RCP2.6, the annual mean precipitation is projected to increase by about +0.13 to +0.37 mm d^{-1}. These precipitation increases are meaningful at the 5-10% significance levels, except for the result of GRIMs. In other RCP scenarios, the annual mean precipitation is projected to change by about −0.01 to +0.31 mm d^{-1}, but it is not significant, except in some results (e.g., WRF: +0.31 mm d^{-1} under RCP4.5, WEA_Tay: +0.19 mm d^{-1} under RCP4.5). As mentioned above, the summer precipitation over South Korea is projected to increase in the southern area, whereas it is projected to decrease in the central area, and as a result, the spatial variability of summer precipitation is projected to be intensified. It is the main reason for the low significance of changes in area-averaged summer precipitation over South Korea. In winter, the precipitation change is relatively small and insignificant compared to that in other seasons.

Figure 9 shows changes in seasonal variation of monthly mean precipitation in the mid-21st century over South Korea compared with the present climate according to the four RCP scenarios. In general, there is a good agreement between HadGEM2-AO and RCM patterns of seasonal precipitation changes, indicating boundary forcing is a major factor. Interestingly, precipitation in July for the mid-21st century is projected to decrease by about −1.0 to −1.8 mm d^{-1} compared to present precipitation in all scenarios, models and ensembles. However, the interannual variability of precipitation in July is projected to become much smaller by about 0.6-0.8 times than present precipitation. Furthermore, the precipitation in June and August is projected to increase by about +0.5 to +1.0 mm d^{-1}. However, the precipitation in June has an interannual variability similar to that of present precipitation, whereas the interannual variability of precipitation in August varies according to the scenarios and ensembles. The amount of precipitation in August is projected to increase by about +1.0 mm d^{-1} in both EWA_NBC and WEA_Tay under RCP4.5, but only the interannual variability of WEA_Tay is expected to become much larger by about 1.5 times than that of the present precipitation. On the other hand, the amount of precipitation in December is projected to be similar to that of present precipitation in all scenarios, but the interannual variability is projected to be much larger by about 1.3 to 1.9 times according to the scenarios and ensembles.

Figure 10 shows changes in the PDF of monthly mean precipitation (mm d^{-1}) in the mid-21st century over South Korea compared with the present period. The results projected by HadGEM2-AO, RegCM4, and two ensembles are presented according to the four RCP scenarios. The frequency of occurrence with precipitation intensity from 0.1 to 3.0 mm d^{-1} is projected to decrease in all models and scenarios, particularly under RCP2.6. On the other hand, the changes for strong precipitation (≥ 15 mm d^{-1}) vary according to the models and scenarios. HadGEM2-AO projects that strong precipitations will be decreased under RCP8.5, but it will be increased under RCP2.6. Similar changes appear in the results of RegCM4. WEA_Tay and EWA_NBC project that the strong precipitations will be increased in all scenarios when compared with the present precipitation. Overall, these contrasting changing patterns, decreasing light precipitation and increasing strong precipitation, are similar to that in previous studies that analyzed precipitation changes in the mid-21st century using RCMs (Im and Kwon, 2007; Lee et al., 2014; Oh et al., 2014; Ham et al., 2015). The differences in changes in precipitation characteristics among RCP scenarios over South Korea are not significant until the mid-21st century. In addition, the relationship between the increase of precipitation and intensity of the net radiative forcing is not linear.

(2) Precipitation changes in the late 21st century

Figure 11 shows changes (%) in the spatial distribution of summer (JJA) and winter (DJF) mean precipitation during the late 21st century (2076-2100) compared with the present period (1981-2005) based on RCP4.5 and RCP8.5 scenarios. As similar to previous studies using GCMs of CMIP5 (e.g., IPCC, 2013; Hsu et al., 2013; Seo et al., 2013), the HadGEM2-AO projects that summer and winter precipitation will be significantly increased in most of Northeast Asia, particularly under RCP8.5. Generally, multi-RCM ensembles project large-scale changes in patterns similar to that of HadGEM2-AO. However, different changes in patterns in some regions, such as Gulf of Pohai and East Sea in North Korea are found during winter. Under RCP4.5, the multi-RCM ensembles project that the summer precipitation around the northern and southern region of the Korean Peninsula, Japanese Islands, and the East China Sea will be significantly increased by about +10% to +30% within the 10% or 1% significance level. The winter precipitation around South Korea and some regions in Japan, and southeastern China is also expected to increase within the 10% significance level. Unlike HadGEM2-AO, the multi-RCM ensembles project large decreases in winter precipitation around the Gulf of Pohai and East Sea in North Korea within 10% significance level similar to that in the mid-21st century. Under RCP8.5, the precipitation change pattern is similar to that under RCP4.5, but the magnitude of precipitation change (%) is projected to be higher. However, the inter-RCM spread is also projected to be larger under RCP8.5 than RCP4.5, particularly around eastern China during the winter. In addition, the magnitude of inter-RCM spread is projected to be larger in the late 21st century than in the mid-21st century. It indicates that the uncertainties for precipitation change among RCMs can be larger with an increase in simulation time and radiative forcing intensity. Therefore, the projected precipitation changes should be used with caution.

To understand the cause of precipitation changes over Northeast Asian region in the late 21st century (2076-2100), we analyzed the changes of wind field (m s^{-1}) and air temperature (°C) at 850 hPa during summer (JJA) and winter (DJF) under the RCP4.5 and RCP8.5 scenarios relative to the present climate (1981-2005) (Fig. 12). Larger precipitation increases occur during summer under RCP8.5 than RCP4.5 (Fig. 11) and are associated with an enhanced southwesterly wind at 850 hPa in most regions of the RCM domain (Figs. 12b, d). Consequently, the inflow of moisture under RCP8.5 is projected to be enhanced compared to present climate and RCP4.5 (not shown). In contrast, under RCP4.5, an enhanced northeasterly wind component is identified around the middle

Table 2. Same as Table 1 except for in the late 21st century (2076-2100).

Seasons	Scenarios	HadGEM2-AO	HadGEM3-RA	RegCM4	GRIMs	WRF	SNU RCM	EWA_NBC	WEA_Tay	Spread of RCMs
Annual	RCP2.6	0.16 (5.4)	0.16 (4.5)	0.28** (5.5)	−0.40 (−11.9)	0.59*** (14.9)	0.30** (9.2)	0.19* (5.3)	0.18* (6.5)	0.36 (10.0)
	RCP4.5	0.11 (3.7)	0.22 (6.3)	0.25** (4.4)	0.31** (9.2)	0.50*** (12.9)	0.30* (8.9)	0.32** (9.5)	0.31** (10.2)	0.11 (3.22)
	RCP6.0	0.10 (3.4)	0.30** (8.7)	0.24 (4.1)	−0.38 (−11.3)	0.31* (8.1)	0.20 (6.2)	0.14 (4.2)	0.14 (4.9)	0.29 (8.28)
	RCP8.5	0.40*** (13.6)	0.52*** (15.6)	0.52*** (13.7)	0.40*** (11.9)	0.86*** (21.8)	0.72*** (21.4)	0.60*** (17.8)	0.59*** (19.1)	0.18 (4.51)
Summer	RCP2.6	−0.29 (−5.5)	0.61 (9.8)	0.70* (9.5)	−1.23 (−19.1)	1.33** (19.7)	1.06** (16.7)	0.49 (7.9)	0.55* (8.5)	1.01 (15.41)
	RCP4.5	0.33 (6.2)	0.73 (11.7)	0.53 (6.6)	0.81** (12.4)	1.15** (17.2)	1.07** (16.9)	0.86** (13.7)	0.84** (12.6)	0.25 (4.35)
	RCP6.0	0.11 (1.9)	0.46 (7.4)	0.24 (1.3)	−1.48 (−23.0)	0.28 (4.3)	0.49 (7.7)	0.00 (0.0)	0.02 (0.8)	0.83 (12.87)
	RCP8.5	0.80* (15.0)	1.20** (19.2)	1.14** (17.6)	0.79* (12.3)	1.90*** (28.2)	2.05*** (32.1)	1.41*** (22.7)	1.39*** (20.5)	0.54 (8.09)
Winter	RCP2.6	0.25* (19.2)	0.04 (3.5)	0.13 (6.3)	0.01 (0.6)	0.20 (8.9)	0.06 (4.0)	0.09 (6.0)	0.07 (9.7)	0.08 (3.12)
	RCP4.5	0.01 (0.8)	0.15 (13.0)	0.19* (11.1)	0.09 (5.8)	0.30** (14.0)	0.04 (2.6)	0.15 (10.6)	0.16 (17.2)	0.10 (4.90)
	RCP6.0	0.04 (2.3)	0.24* (20.9)	0.16 (7.9)	−0.10 (−6.5)	0.12 (5.6)	−0.01 (−1.3)	0.08 (5.3)	0.09 (9.7)	0.14 (10.40)
	RCP8.5	0.22* (16.9)	0.39** (33.9)	0.29** (19.0)	0.14 (9.7)	0.52*** (24.3)	0.20* (13.2)	0.31** (20.5)	0.31** (33.3)	0.15 (9.55)

***Significance level: 1%, **Significance level: 5%, *Significance level: 10%

region of the Korean Peninsula. It indicates that the summer monsoon circulation will be shifted toward the Southern Ocean in Japan. Therefore, a greater precipitation increase is projected around the East China Sea including southern South Korea, but a precipitation decrease is projected in the middle region of the Korean Peninsula. The precipitation decreases during winter around the Gulf of Pohai and the East Sea in North Korea are associated with an enhanced northwesterly wind and different warming trends compared to the present climate. That is, more warming trend in northeastern China relative to the Gulf of Pohai and the East Sea in North Korea may induce a stabilization of vertical structure with enhanced cold advection by an increase in northwesterly wind in these regions. The precipitation increases during the winter around southeastern China, South Korea, and East Sea in Korea seem to be related to the reinforcement of a westerly or southwesterly wind.

The amount of change (mm d^{-1}) in seasonal mean precipitation during the late 21st century compared with the present period over South Korea according to the four RCP scenarios are summarized in Table 2. The amount of change in precipitation over South Korea varies according to seasons, models or ensembles, and RCP scenarios. The annual and summer mean precipitations are expected to increase at a 5% significance level, but the winter precipitation change is not significant, except for that under RCP8.5. Increase amount (ratio) in the annual mean precipitation projected by WEA_Tay for the late 21st century according to the four RCP scenarios is as follows: about +0.18 mm d^{-1} (+6.5%) under RCP2.6, +0.31 mm d^{-1} (+10.2%) under RCP4.5, +0.14 mm d^{-1} (+4.9%) under RCP6.0, and +0.59 mm d^{-1} (+19.1%) under RCP8.5. These changes are meaningful at 1 to 5% significance levels, except for under RCP6.0. In particular, under RCP8.5, all models including HadGEM2-AO project that the annual mean precipitation will be increased by about +0.40 to +0.86 mm d^{-1} at a 1% significance level. In summer, an increase in precipitation is projected in all scenarios, except for RCP6.0. Under RCP8.5, WEA_Tay projects that summer precipitation will be increased by about +1.39 mm d^{-1} (+20.5%). On the other hand, the change in winter precipitation is not significant in the most scenarios. However, the increase in precipitation under RCP8.5 is expected to be about +0.31 mm d^{-1} (+33.3%) at 5% significance level due to increased precipitation in the southwestern area of South Korea.

Figure 13 shows changes in seasonal variation of monthly mean precipitation in the late 21st century over South Korea compared with the present period according to the four RCP scenarios. Generally, the changes of monthly mean precipi-

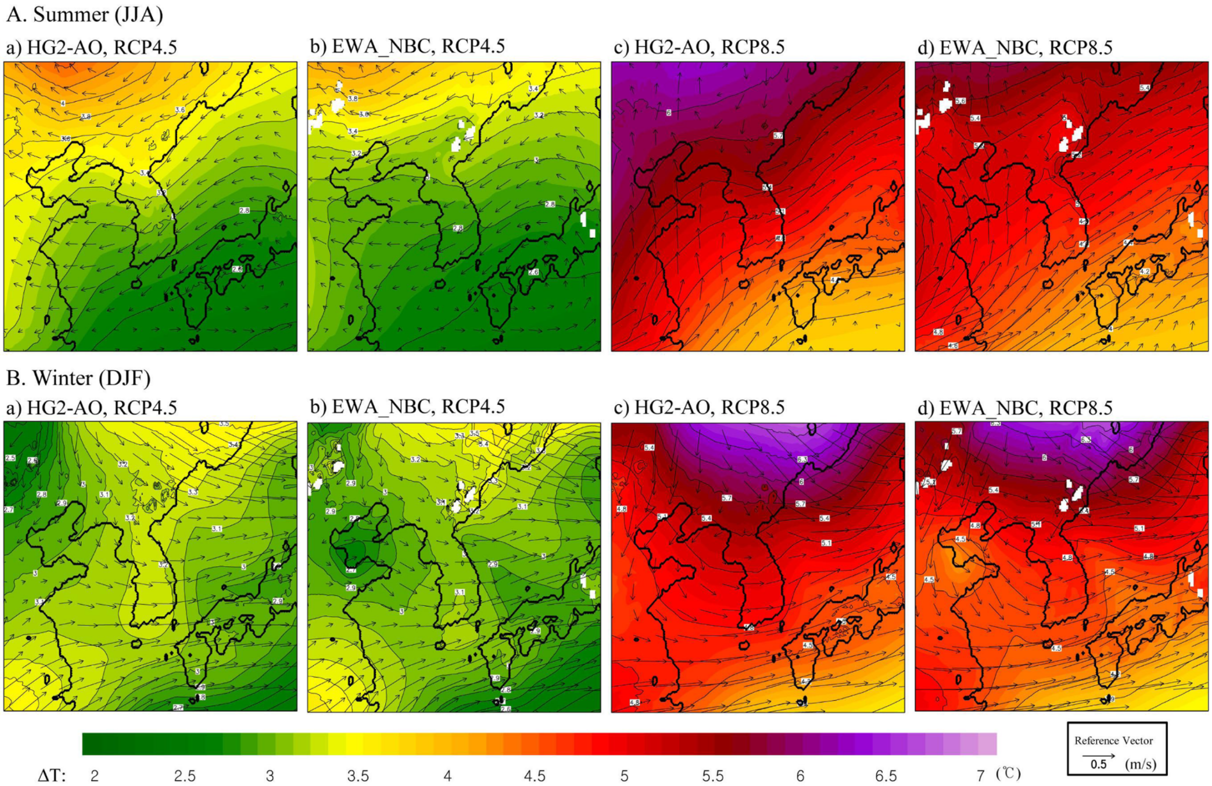

Fig. 12. Change of spatial distribution of wind field (m s^{-1}) and temperature (^{o}C) at 850 hPa in the late 21st century (2076-2100) compared to the modeled present climate (1981-2005) under RCP4.5 and 8.5 scenarios during summer (JJA) and winter (DJF).

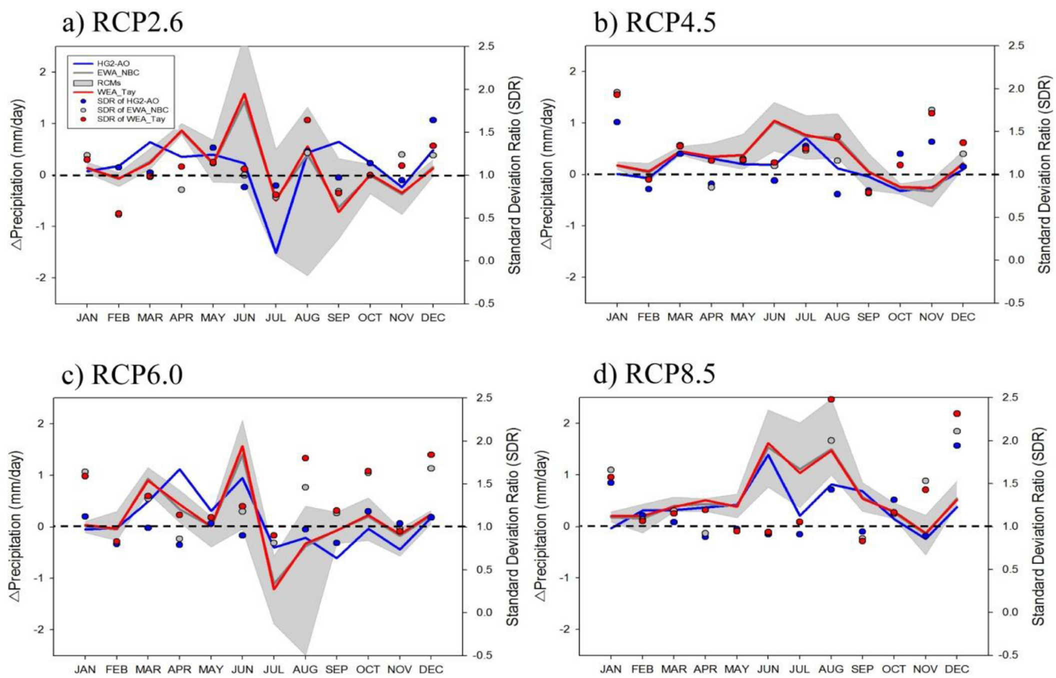

Fig. 13. Same as Fig. 9 except for in the late 21st century (2076-2100).

tation over South Korea show large differences according to RCP scenarios, unlike the results in the mid-21st century. Under RCP2.6 and RCP6.0, the precipitation in spring (e.g., Apr. under RCP2.6 and Mar. under RCP6.0) and June are

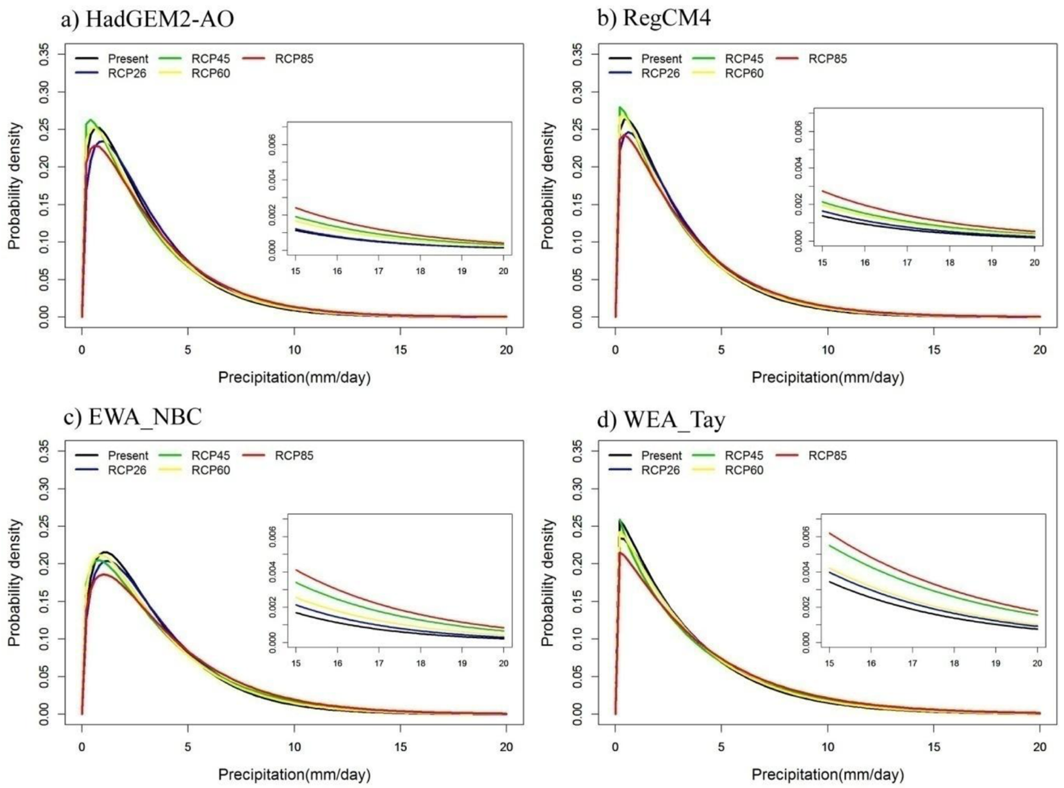

Fig. 14. Same as Fig. 10 except for in the late 21st century (2076-2100).

projected to clearly increase, but that in July is projected to decrease. WEA_Tay projects the precipitation in July to significantly decrease by about -1.0 mm d^{-1} when compared with the present precipitation. Under RCP4.5 and RCP8.5, most of the monthly precipitations are projected to increase, particularly in June and August, except for that in autumn (e.g., Oct. and Nov. under RCP4.5, and Nov. under RCP8.5). The precipitation in August is especially expected to increase the interannual variability by about 1.5 times (up to a maximum of 2.5 times under RCP8.5) compared to present precipitation. In addition, the interannual variability for winter precipitation is expected to increase by about 1.3 times (up to a maximum 2.3 of times under RCP8.5). These increases in interannual variability of monthly precipitation in the late 21st century are relatively much larger than that in the mid-21st century (Fig. 9), particularly under RCP8.5. This indicates that the probability of abnormal precipitation events, such as drought and flood, might be more significant in the late 21st century compared to the present and mid-21st century. In addition, taking into account the fact which the precipitation in August is associated with the development of the mesoscale convective system, the increase in interannual variability for the precipitation in August can indicate the increase in interannual variability for the development of mesoscale convective systems.

Similar to Fig. 10, Fig. 14 shows changes in the PDF of monthly mean precipitation (mm d^{-1}) in the late 21st century over South Korea compared with the present period. Overall, all models and ensembles project that light precipitation (0.1-3.0 mm d^{-1}) will be decreased, but strong precipitation ($\geq$ 15.0 mm d^{-1}) will be increased. In particular, increases in strong precipitation are projected to be much larger than that in the mid-21st century. This means that the occurrence probability of extreme precipitation will be much higher in the late 21st century than in the mid-21st century, regardless of RCP scenarios. In addition, more increase in the occurrence frequency of strong precipitation is projected under RCP8.5 than the other RCP scenarios, unlike during the mid-21st century. The rate of changes in the occurrence probability for precipitation (15-20 mm d^{-1}) for the late 21st century according to the four RCP scenarios varies among models and ensembles. In general, two ensembles showed more increase; in particular, WEA_Tay projects that the probability of strong precipitation will be much higher by about 1.5-3.0 times than the other models and EWA_NBC.

4. Summary

In this study, we evaluated the performance of the five RCMs (HadGEM3-RA, RegCM4, GRIMs, WRF, and SNURCM) and two ensemble methods (EWA_NBC, WEA_Tay) for the present (1981-2005) precipitation over the Northeast Asian region focusing on the Korean Peninsula. Furthermore, we projected changes in precipitation for the mid (2026-2050) and late (2076-2100) 21st century under the four RCP scenarios (2.6, 4.5, 6.0, and 8.5). Simulation data of HadGEM2-AO, provided by the NIMS/KMA, was used as boundary data for the five RCMs. To validate the performance of precipitation for the present period, the APHRODITE precipitation data based on surface observation was used.

In general, all the five RCMs simulate the spatial and temporal variations of precipitation relatively better than that of HadGEM2-AO, although they systematically underestimate the amplitude of seasonal variation for monthly precipitation compared with APHRODITE. In particular, they show better performances in the simulation of strong precipitation (≥ 15 mm d^{-1}) than HadGEM2-AO. EWA_NBC shows a good performance in terms of bias, RMSE, and spatial correlation compared with each RCM, but it still shows unresolved bias characteristics which appear systematically in the RCM results. In contrast, WEA_Tay shows a good statistical correction in terms of the bias, correlation, RMSE, and probability density. It indicates that statistical correction is needed for the analysis and projection of mean and extreme climate.

In the mid-21st century, regardless of RCP scenarios, the precipitation is projected to increase in the southern area of the Korean Peninsula, the East China Sea, but to decrease in the central area of the Korean Peninsula. As the results, the spatial gradient of precipitation is projected to intensify in all scenarios. The increase or decrease of the amount and interannual variability of monthly precipitation is insignificant and projected to vary according to months. In addition, the relationship between the increase of precipitation and intensity of radiative forcing does not show a linearity trend in the mid-21st century.

In the late 21st century, precipitation is projected to increase proportional to the changes of net radiative forcing, and the changes of precipitation over South Korea are significant in most RCP scenarios at 1-5% significance levels. Under RCP8.5, WEA_Tay projects that the annual, summer, and winter mean precipitation over South Korea are significantly increased by about +0.59 mm d^{-1} (+19.1%), +1.39 mm d^{-1} (+20.5%), and +0.31 mm d^{-1} (+33.3%), respectively, compared with the present period (1981-2005). The interannual variability of monthly precipitation and the frequency of strong precipitation (≥ 15 mm d^{-1}) over South Korea in the late 21st century are projected to increase much larger than that in the present and the mid-21st century. In particular, WEA_Tay projects that the probability of strong precipitation will be much higher by about 1.5-3.0 times than the other RCMs and EWA_NBC according to RCP scenarios.

5. Conclusions

This is the first study to evaluate present precipitation and to project precipitation changes for the mid and late 21st century over Northeast Asian region based on four RCP scenarios using two multi-RCM ensembles. The precipitation increases (%) in the late 21st century (2076-2100) over South Korea projected from this work are generally larger than the corresponding the changes over East Asia and global region, with greater differences under RCP 8.5 (e.g., Hsu et al., 2013; IPCC, 2013; Seo et al., 2013; Xin et al., 2013). Unlike temperature changes by Suh et al. (2016) as a companion study, the precipitation increases (%) of multi-RCM ensembles are generally larger than that of HadGEM2-AO in most seasons and scenarios. The smaller temperature increases over South Korea in the multi-RCM ensembles compared to HadGEM2-AO (Suh et al., 2016) are partly related to greater precipitation increases. As the evaluation results for present climate indicated, the multi-RCM ensembles can improve the performance of precipitation over Northeast Asian region, particularly when using WEA_Tay. However, the projected results of this study, including WEA_Tay for the mid and late 21st century, should be used with caution because we assumed that the "stationarity", the performance of RCMs did not change with time. In addition, under RCP4.5, the precipitation change which looks like decadal or inter-decadal variation (Fig. 7b) can also bring another uncertainty to the projection of the mid and late 21st century. Therefore, to understand the precipitation changes and their uncertainties induced by various factors (lateral boundary data, RCMs, climate scenarios, etc.), an in-depth analysis including a study of the involved mechanisms is needed (e.g., Zou and Zhou, 2013). Moreover, a detailed analysis of the changes in the characteristics of extreme events is also needed because the impacts of climate change are mostly derived from the changes in pattern of extreme events. Finally, previous studies suggest that the performance of ensembles is improved when ensemble members consist of independent multi-GCMs and multi-RCMs (e.g., Giorgi and Mearns, 2002; Yun et al., 2005; Casanova and Ahrens, 2009; Suh et al., 2012; Oh and Suh, 2015). Therefore, various simulation dataset produced from multi-RCMs forced by multi-GCMs are required to produce more reliable climate change information from ensembles.

Acknowledgements. This work was funded by the Korea Meteorological Administration Research and Development Program under Grant KMIPA 2015-2084.

Edited by: Tianjun Zhou

References

Baek, H. J, and Coauthors, 2013: Climate change in the 21st century simulated by HadGEM2-AO under representative concentration pathways. *Asia-Pac. J. Atmos. Sci.*, **49**, 603-618.

Bao, Q., 2012: Projected changes in Asian summer monsoon in RCP scenarios of CMIP5. *Atmos. Oceanic Sci. lett.*, **5**, 43-48.

Byun, Y. H., and S. Y. Hong, 2007: Improvements in the subgrid-scale representation of moist convection in a cumulus parameterization scheme: The single-column test and its impact on seasonal prediction. *Mon. Wea. Rev.*, **135**, 2135-2154.

Casanova, S., and B. Ahrens, 2009: On the weighting of multimodel ensembles in seasonal and short-range weather forecasting. *Mon. Wea. Rev.*, **137**, 3811-3822.

Christensen, J. H., E. Kjellström, F. Giorgi, G. Lenderink, and M.

Rummukainen, 2010: Weight assignment in regional climate models. *Clim. Res.*, **44**, 179-194.

Collins, W. J., and Coauthors, 2011: Development and evaluation of an Earth-system model - HadGEM2. *Geosci. Model Dev. Discuss*., **4**, 997-1062.

Dodla, V. B. R., S. B. Ratna, and S. Desametti, 2013: An assessment of cumulus parameterization schemes in the short range precipitation of rainfall during the onset phase of the Indian Southwest Monsoon using MM5 Model. *Atmos. Res.*, **120-121**, 249-267.

Easterling, D. R., G. A. Meehl, C. Parmesan, S. A. Changnon, T. R. Karl, and L. O. Mearns, 2000: Climate extreme: observation, modeling, and impacts. *Science*, **289**, 2068-2074.

Emanuel, K. A., 1991: A scheme for representing cumulus convection in large-scale models. *J. Climate*, **48**, 2313-2335.

Fu, C., S. Wang, Z. Xiong, W. Gutowski, D. K. Lee, J. L. Mc-Gregor, Y. Sato, H. Kato, J.-W. Kim, and M.-S. Suh, 2005: Regional climate model intercomparison project for Asia. *Bull. Amer. Meteor. Soc.*, **77**, 437-471.

Giorgi, F., and L. O., Mearns, 1999: Introduction to special section: regional climate modeling revisited. *J. Geophys. Res.,* **104**, 6335-6352.

______, and ______, 2002: Calculation of average, uncertainty range, and reliability of regional climate changes from AOGCM simulations via the 'reliability ensemble averaging' (REA) method. *J. Climate,* **15**, 1141-1158.

______, and Coauthors, 2012: RegCM4: model description and preliminary test over multi CORDEX domains. *Clim. Res.*, **52**, 7-29.

Gregory, D., and P. R. Rowntree, 1990: A mass flux convection scheme with representation of cloud ensemble characteristics and stability-dependent closure. *Mon. Wea. Rev.*, **118**, 1483-1506.

Gu, H., G. Wang, Z. Yu, and R. Mei, 2012: Assessing future climate changes and extreme indicators in east and south Asia using the RegCM4 regional climate model. *Climatic Change*, **114**, 301-317.

Ham, S., J. W. Lee, and K. Yoshimura, 2015: Assessing future climate changes in the East Asian summer and winter monsoon using regional spectral model. *J. Meteor. Soc. Japan*, **92**, 69-87.

Hewitt, H. T., D. Copsey, I. D. Culverwell, C. M. Harris, R. S. R. Hill, A. B. Keen, A. J. McLaren, and E. C. Hunke, 2010: Design and implementation of the infrastructure of HadGEM3: the next-generation Met Office climate modeling system. *Geosci. Model Dev. Discuss.*, **3**, 1861-1937.

Hong, J. Y., and J. B. Ahn, 2015: Changes of early summer precipitation in the Korean peninsula and nearby regions based on RCP simulations. *J. Climate*, **28**, 3557-3578.

Hong, S. Y., and H. L. Pan, 1998: Convective trigger function for a mass flux cumulus parameterization scheme. *Mon. Wea. Rev.*, **126**, 2599-2620.

______, and Coauthors, 2013: The global/regional integrated model system (GRIMs). *Asia-Pac. J. Atmos. Sci*., **49**, 219-243.

Hsu, P., T. Li, H. Murakami, and A. Kitoh, 2013: Future change of the global monsoon revealed from 19 CMIP5 models. *J. Geophy. Res.*, **118**, 1247-1260.

Im, E. S., and W. T. Kwon, 2007: Characteristics of extreme climate sequences over Korea using regional climate change scenario. *SOLA*, **3**, 17-20.

IPCC, 2013: *Climate Change 2013: The Physical Science Basis.* Cambridge University Press, 1535 pp.

Jacob, D., and Coauthors, 2007: An inter-comparison of regional climate models for Europe: model performance in present-day climate. *Climatic Change*, **81**, 31-52.

Jeong, D. I., L. Sushama, and M. N. Khaliq, 2014: The role of temperature in drought projections over North America. *Climatic Change*, **127**, 289-303.

Ji, Z., and S., Kang, 2014: Evaluation of extreme climate events using a regional climate model for China. *Int. J. Climatol*., **35**, 888-902.

Jin, C. S., D. H. Cha, D. K. Lee, M. S. Suh, S. Y. Hong, H. S. Kang, and C. H. Ho, 2015: Evaluation of climatological tropical cyclone activity over the western North Pacific in the CORDEX East Asia multi-RCM simulations. *Clim. Dynam*., doi:10.1007/s00382-015-2869-6.

Kain, J. S., 2004: The Kain-Fritsch convective parameterization: An update. *J. Appl. Meteorol.*, **43**, 170-181.

______, and J. M. Fritsch, 1993: Convective parameterization for mesoscale models: The Kain-Fritsch scheme. In *The presentation of cumulus convection in numerical models*, Amer. Meteorol. Soc., 246 pp.

Kerkhoven, E., T. Y. Gan, M. Shiiba, G. Reuter, and K. Tanaka, 2006: A comparison of cumulus parameterization schemes in a numerical weather prediction model for a monsoon rainfall event. *Hydrol. Process.*, **20**, 1961-1979.

Kim, C. S., M. S. Suh, and K. O. Hong, 2009: Bayesian change point analysis of the annual maximum of daily and sub-daily precipitation over South Korea. *J. Climate*, **22**, 6741-6757.

Klein Tank, A. M. G., and G. P. Können, 2003: Trend in indices of daily temperature and precipitation extremes in Europe. *J. Climate*, **16**, 3665-3680.

KMA, 2015: Production of fine-scale climate change data over the Korean peninsula using RCP scenarios. Research report (CATER 2012-3080), 822 pp.

Krishnamurti, T. N, C. M. Kishtawal, T. LaRow, D. Bachiochi, Z. Zhang, E. Williford, S. Gadgil, and S. Surendran, 1999: Improved weather and seasonal climate forecasts from multimodel superensemble. *Science*, **285**, 1548-1550.

Lee, D. K., and M. S. Suh, 2000: Ten-year East Asian summer monsoon simulation using a regional climate model (RegCM2). *J. Geophys. Res.*, **105**(D24), 29565-29577.

______, D. H., Cha, and H. S. Kang, 2004: Regional climate simulation for the 1998 summer flood over East Asia. *J. Meteor. Soc. Japan,* **82,** 1735-1753.

Lee, J. W., S. Y. Hong, E. C. Chang, M. S. Suh, and H. S. Kang, 2014: Assessment of future climate change over East Asia due to the RCP scenarios downscaled by GRIMs-RMP. *Clim. Dynam*., **42**, 733-747.

Li, Q., and Coauthors, 2016: Building Asian climate change scenario by multi-regional climate models ensemble. Part II: mean precipitation. *Int. J. Clmatol.*, doi:10.1002/joc.4633.

Litta, J., B. Chakrapani, and K. Mohankumar, 2007: Mesoscale simulation of an extreme rainfall event over Mumbai, India, using a high resolution MM5 model. *Meteorol. Appl.*, **14**, 291-295.

Meehl, G. A., G. J. Boer, C. Covey, M. Latif, and R. J. Stouffer, 2000: The coupled model intercomparison project (CMIP). *Bull. Amer. Meteor. Soc.*, **81**, 313-318.

Moss, R., and Coauthors, 2008: Towards new scenarios for analysis of emissions, climate change, impacts, and response strategies. *Technical Summary*, *Intergovernmental Panel on Climate Change*, Geneva, 25 pp.

Oh, S. G., J. H. Park, S. H. Lee, and M. S. Suh, 2014: Assessment of the RegCM4 over East Asia and future precipitation change adapted to the RCP scenarios. *J. Geophys. Res. Atmos.*, **119**, 2913-2927.

______, and M. S. Suh, 2015: Comparison of projection Skills of deterministic ensemble methods using pseudo-simulation data generated from multivariate Gaussian distribution. *Theor. Appl. Climatol.*, doi: 10.1007/s00704-016-1782-1.

______, ______, D. H. Cha, and S. J. Cho, 2011: Simulation skills of RegCM4 for regional climate over CORDEX East Asia driven by HadGEM2-AO. *J. Korean Earth Sic. Soc.*, **32**, 732-749 (in Korean with English abstract).

Palmer, T. N., and Coauthors, 2004: Development of a European multi-model ensemble system for seasonal to interannual prediction (DEMETER). *Bull. Amer. Meteor. Soc.*, **85**, 853-872.

Park, C., S. K. Min, D. Lee, D. H. Cha, and M. S., Suh, 2015: Evaluation of multiple regional climate models for summer climate extremes over East Asia. *Clim. Dynam*., doi:10.1007/s00382-015-2713-z.

Skamarock, W. C., J. B. Klemp, J. Dudhia, D. O. Gill, D. M. Barker, W. Wang, and J. G. Powers, 2005: A description of the Advanced Research WRF version 2. NCAR Tech. Note. NCAR/TN-468+STR, National Center for Atmospheric Research, Boulder, CO, 100 pp.

Seo, K. H., J. Ok, and J. H. Son, 2013: Assessing future change in the East Asian summer monsoon using CMIP5 coupled models. *J. Climate*, **26**, 7662-7675.

Suh, M. S., and D. K. Lee, 2004: Impacts of land use/cover changes on surface climate over East Asia for extreme climate cases using RegCM2. *J. Geophys. Res.*, **109**(D2), doi:10.1029/2003JD003681.

______, S. G. Oh, Y. S. Lee, J. B. Ahn, D. H. Cha, D. K. Lee, S. K. Min, S. C. Park, and H. S. Kang, 2015: Projections of high resolution climate changes for South Korea using multiple-regional climate models based on four RCP scenarios. Part 1: Surface air temperature. *Asia-Pac. J. Atmos. Sci*., **52**(2), doi:10.1007/s13143-016-0017-9.

______, ______, D. K. Lee, D. H. Cha, S. J. Choi, C. S. Jin, and S. Y. Hong, 2012: Development of new ensemble methods based on the performance skills of regional climate models over South Korea. *J. Climate*, **25**, 7067-7082.

Sung, J. H., H. S. Kang, S. Park, C. H. Cho, D. H. Bae, and Y. O. Kim, 2012: Projection of extreme precipitation at the end of 21st century over South Korea based on representative concentration pathways (RCP). *Atmosphere*, **22**, 221-231 (in Korean with English abstract).

Taylor, K. E., 2001: Summarizing multiple aspects of model performance in a single diagram. *J. Geophys. Res.*, **106**(D7), 7183-7192.

______, R. J. Stouffer, and G. A. Meehl, 2012: An Overview of CMIP5 and the Experiment Design. *Bull. Am. Meteor. Soc.*, **93**, 485-498.

Van der Linden, P., and J. F. Mitchell, 2009: ENSEMBLES: Climate change and its impacts: Summary of research and results from the ENSEMBLES project. Met Office Hadley Centre Tech. Rep., 160 pp.

Van Vuuren, D. P., and Coauthors, 2011: The representative concentration pathways: an overview. *Climatic Change*, **109**, 5-31.

Wang, S.-Y., R. R. Gillies, E. S. Takle, and W. J. Gutowski Jr., 2009: Evaluation of precipitation in the inter-mountain region as simulated by NARCCAP regional climate models. *Geophys. Res. Lett.*, **36**, L11704, doi:10.1029/2009GL037930.

Yatagai, A., K. Kamiguchi, O. Arakawa, A. Hamada, N. Yasutomi, and A. Kitoh, 2012: APHRODITE: Constructing a long-term daily gridded precipitation dataset for Asia based on a dense network of rain gauges. *Bull. Amer. Meteor. Soc.*, **93**, 1401-1415.

Yoon, J. H. K. Mo, and E. F. Wood, 2012: Meteorological drought prediction based on the standard precipitation index. *J. Hydrometeorology*, **13**, 463-482.

Yun, W. T., A. K. Mitra, T. S. V. V. Kumar, W. Dewar, and T. N. Krishnamurti, 2005: A multi-model synthetic superensemble algorithm for seasonal climate prediction using DEMETER forecasts. *Tellus*, **57**, 280-289.

Zou, L., and T. Zhou, 2013: Near-future (2016-2040) summer precipitation changes over China as projected by a regional climate model (RCM) under the RCP8.5 scenario: Comparison between RCM downscaling and the driving GCM. *Adv. Atmos. Sci.*, **20**, 806-818.